Molecular and Cellular Biochemistry 50, 47–64 (1983)

Alamethicin and related membrane channel forming polypeptides

M. K. Mathew and P. Balaram
Molecular Biophysics Unit, Indian Institute of Science, Bangalore-560 012, India

Summary

Alamethicin and several related microbial polypeptides, which contain a high proportion of α-aminoisobutyric acid (Aib) residues, possess the ability to modify the permeability properties of phospholipid bilayer membranes. Alamethicin induces excitability phenomena in model membranes and has served as an excellent model for the study of voltage sensitive transmembrane channels. This review summarizes various aspects of the structural chemistry and membrane modifying properties of alamethicin and related Aib containing peptides. The presence of Aib residues in these sequences, constrains the polypeptides to 3_{10} or α-helical conformations. Functional membrane channels are formed by aggregation of cylindrical peptide helices, which span the lipid bilayer, forming a scaffolding for an aqueous column across the membrane. After consideration of the available data on the conductance characteristics of alamethicin channels, a working hypothesis for a channel model is outlined. Channel aggregates in the lipid phase may be stabilized by intermolecular hydrogen bonding, involving a central glutamine residue and also by interactions between the macro-dipoles of proximate peptide helices. Fluctuations between different conductance states are rationalized by transitions between states of different aggregation and hence altered dimensions of the aqueous core or by changes in net dipole moment of the aggregate. Ion fluxes through the channel may also be affected by the electric field within the aqueous core.

Introduction

The transport of ions and neutral molecules across lipid bilayer membranes may be mediated by diffusible carriers or by formation of transmembrane channels or pores (1, 2). The study of specific transport systems in intact cells and organelles has been hampered by the complexity of their structural organization and difficulties in their isolation and reconstitution into model membranes (3, 4). The understanding of the structural and mechanistic characteristics of carrier and channel mediated membrane transport has been largely based on studies of membrane active antibiotics elaborated by bacterial systems (5, 6). While considerable attention has been focussed over the past two decades on the structural basis of cation selectivity of carrier ionophores, with the cyclic depsipeptide valinomycin being the best studied example (6–8), the study of membrane channels has been developed more recently and is currently an area of intense activity (9–12).

The channel forming antibiotics can be classified into two groups:

1) Channels yielding linear current voltage curves (voltage insensitive conductance), like gramicidin A (13), and the polyene antibiotics, nystatin (14) and amphotericin B (15).
2) Channels which exhibit nonlinear current voltage curves (voltage sensitive conductance), like hemocyanin (16), excitability inducing material

(EIM) (17), monazomycin (18), rhodopsin (19), alamethicin (20) and suzukacillin (21).

The best studied of the first class of ionophores is gramicidin A which has L and D amino acids alternating over a considerable portion of its primary structure. It has now been established that the pore consists of a dimer, formed by head to head association of two monomeric π^6-LD helices, in which a central aqueous core is lined with suitably positioned carbonyl groups for interaction with metal ions (22–24). The rate of ion transport is estimated to be $\sim 2 \times 10^6$ ions/channel/s (25). The best fit of the available kinetic data is to a 3 barrier – 4 site model of the channel (26), through which ions move in single file (27–29). This model is based on the assumption of a single "open" state and may require modification in view of the recently reported complexity of gramicidin conduction (30).

The picture regarding voltage sensitive channels is not so clear. While data on the unit conductance events of EIM (31), hemocyanin (16) and alamethicin (32), have been related to their macroconductance data, there is no consensus molecular model for the activity of any voltage sensitive channel forming ionophore. More than one molecule of ionophore is required to form a pore and all available models are based on the arrangement of monomers to form a suitable pore (32–36). These channel formers are of particular interest since single channel conductance experiments on intact biological membrane systems, suggest that protein channels invariably exhibit complex conductance behaviour (37, 38). Further, these ionophores may be used to impart excitability characteristics to artificial lipid membranes (9, 20). The best studied example in this class is alamethicin (9), a polypeptide rich in the unusual amino acid, α-aminoisobutyric acid (Aib). The isolation of a number of closely related, Aib containing, membrane active peptides (39–45) (see Figure 1 for representative examples), has stimulated attempts to build structure–activity correlations for these channel forming polypeptides (46, 47).

Structural chemistry of Aib-containing membrane channels

Early attempts to establish the sequence of alamethicin, isolated from *Trichoderma viride* (48), led to the proposal of a cyclic structure (49, 50), which was later revised to a linear structure, based on 270 MHz ^{1}H NMR studies (51). Sequencing of "alamethicin" was also rendered difficult by the heterogeneity of the natural product, which has recently been separated into at least 12 closely related polypeptides, by HPLC (52). Sequences of the major components (alamethicin I and II) have been proposed on the basis of field desorption mass spec-

Suzukacillin A[39]: Ac-Aib-Pro-Val-Aib-Val-Ala-Aib-Ala-Aib-Aib-Gln-Aib-Leu-Aib-Gly-Leu-Aib-Pro-Val-Aib-Aib-Glu-Gln-Phol

Alamethicin I(II)[40]: Ac-Aib-Pro-Aib-Ala-Aib-Ala(Aib)-Gln-Aib-Val-Aib-Gly-Leu-Aib-Pro-Val-Aib-Aib-Glu-Gln-Phol

Hypelcin A[44]: Ac-Aib-Pro-Aib-Ala-Aib-Aib-Gln-Leu-Aib-Gly-Aib-Aib-Aib-Pro-Val-Aib-Aib-Gln-Gln-Leuol

Trichotoxin A-40[43]: Ac-Aib-Gly-Aib-Ala-Aib-Gln-Aib-Aib-Aib-Ala-Aib-Aib-Pro-Leu-Aib-Iva-Gln-Valol

Emerimicin III(IV)[42]: Ac-Phe-Aib-Aib-Aib-Val-Gly-Leu-Aib-Aib-Hyp-Gln-Iva-Hyp-Ala(Aib)-Phol

Antiamoebin I[41]: Ac-Phe-Aib-Aib-Iva-Gly-Leu-Aib-Aib-Hyp-Gln-Iva-Hyp-Aib-Pro-Phol

Zervamicin IIA[45]: Ac-Trp-Ile-Gln-Aib-Ile-Thr-Aib-Leu-Aib-Hyp-Gln-Aib-Hyp-Aib-Pro-Phol

Fig. 1. Sequences of Aib containing polypeptides that form transmembrane channels.

trometry (40). The identity of a fully synthetic sequence with the major component has been established (52, 53). The Aib containing peptide channels range in length from 15 to 24 residues, with the best characterized member being alamethicin. Several common features are readily apparent in their sequences (Fig. 1). All the peptides have an acetylated amino terminal, an amino alcohol as the C-terminal residue and a long, largely hydrophobic sequence beginning at the N-terminal. The longer peptides (alamethicin, suzukacillin, hypelcin and trichotoxin) are also characterized by a polar C-terminal tail containing Gln, Glu and amino alcohol residues. These molecules also have a Pro residue positioned as the sixth or seventh residue from the C-terminal. The shorter channel formers (emerimicins, zervamicins and antiamoebins) also contain two hydroxyproline residues in the C-terminal segment. Relatively minor replacements (including isovaline for Aib) result in complex mixtures of the natural products. The isolation of a large number of Aib containing channel forming polypeptides, with similar though not identical membrane activity, suggests that common structural principles may be involved in channel organization, with an important role for Aib residues in generating the appropriate polypeptide conformations.

Conformations of Aib peptides

Polypeptide chains are generally composed of all *trans* peptide units, with two degrees of freedom available about the N-C^{α} (ϕ) and C^{α}-CO (ψ) bonds. Various chain conformations may then be generated by varying the values of the torsion angles ϕ and

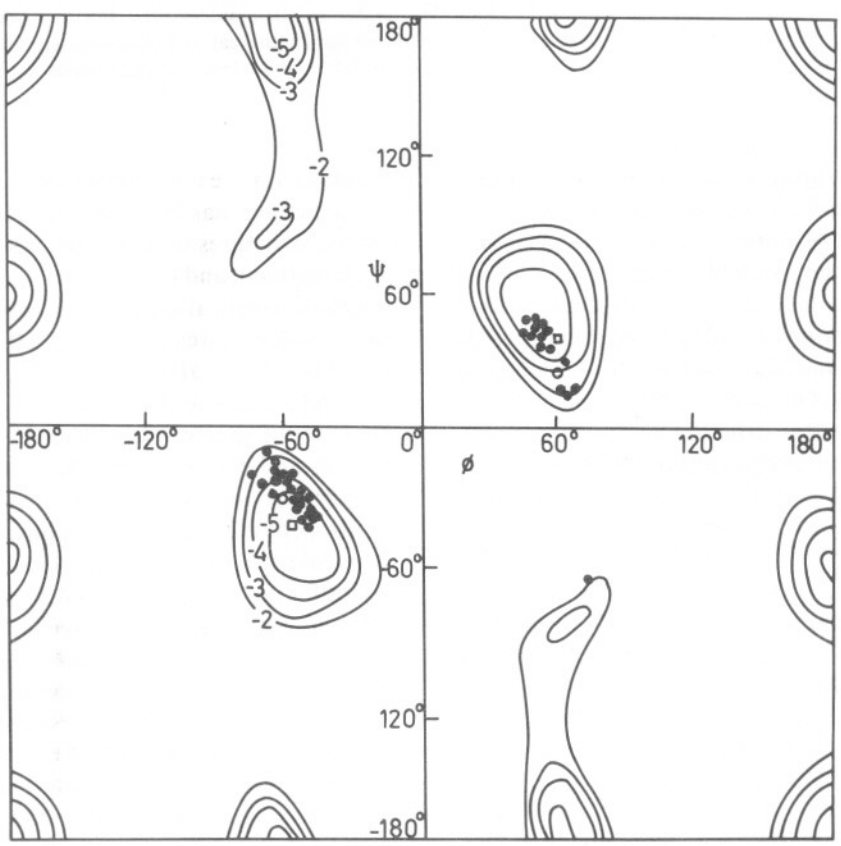

Fig. 2. Potential energy plot of Ac-Aib-NHMe (from reference 56) compared with crystal structure observations of Aib containing peptides (●). The contours are drawn at 1 kcal/mole intervals with respect to the inner most contour enclosing the minimum. The (ϕ, ψ) values of ideal α- and 3_{10} helices (both right and left handed) are represented by □ and ○, respectively.

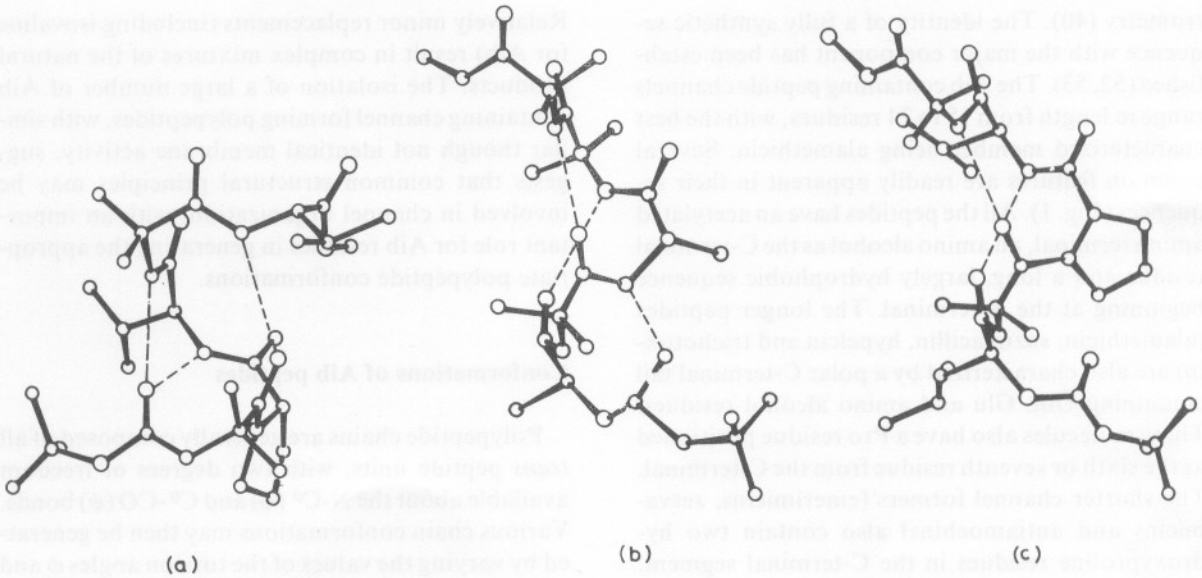

Fig. 3. Solid state conformation of three pentapeptide fragments of suzukacillin determined by x-ray diffraction. a, Boc-Aib-Pro-Val-Aib-Val-OMe (residues 1–5) (68): b, Boc-Ala-Aib-Ala-Aib-Aib-OMe (residues 6–10) (unpublished); c. Boc-Leu-Aib-Pro-Val-Aib-OMe (residues 16–20) (unpublished). The 6–10 and 16–20 segments adopt almost ideal 3_{10} helical conformations stabilized by 4→1 hydrogen bonds. The 1→5 segment adopts a distorted helical structure stabilised by 2 5→1 and 1 4→1 hydrogen bonds.

ψ (54). For Aib residues, theoretical model building and semiempirical energy calculations establish that the presence of geminal methyl groups at C^{α}, greatly restricts the available range of conformations (55–57). From Fig. 2 it is seen that Aib residues are constrained to adopt conformations in the right or left handed 3_{10} and α-helical regions of the conformational map ($\phi \sim \pm 60° \pm 20°$ and $\psi \sim \pm 30° \pm 20°$). Crystal structure analysis of a large number of Aib containing peptides (represented in Figure 2) (58–68), provide strong evidence for this conclusion (46). The solid state helical conformations of pentapeptide fragments of suzukacillin, which correspond to segments 1-5 (68), 6-10 and 16-20 of the ionophore, are illustrated in Fig. 3. The presence of L-amino acids in these peptides results in adoption of right handed (negative ϕ, ψ values) helical conformations.

Both 3_{10} and α-helical structures are stereochemically feasible for Aib containing sequences. There is only a small difference in ϕ, ψ values for these structures and they differ primarily in their hydrogen bonding schemes, with a 4→1 (NH of residue i+3 to CO of residue i) pattern for the 3_{10} helix (69) and a 5→1 pattern for the αhelix (70) (Fig. 4). Evidence for the tendency of Aib peptides to favour 3_{10} structures has been provided by a number of crystal structures of model peptides and fragments of alamethicin and suzukacillin. Conformations resembling α-helical segments have been demonstrated in a model 11-residue peptide (Boc-Ala-Aib-Ala-Aib-Ala-Glu(γ-OBz)-Ala-Aib-Ala-Aib-Ala-OMe) (71) and a suzukacillin fragment (68). A considerable body of spectroscopic (NMR (72–76), IR (73, 77, 78) and CD (73, 79, 80)) data also provides support for the formation of helical structures in solution, by Aib containing fragments of alamethicin, suzukacillin and model peptides. Spectroscopic, crystallographic and theoretical studies, thus favour the formation of relatively rigid helical conformations by Aib containing channel peptides. Neither 3_{10} nor α helical polypeptides can accommodate the passage of ions through the helix interior. Theoretical estimates (81) for passage of H^{+} through the interior of a poly L-alanine α-helix, suggest an energy barrier of ~200 kcal mol^{-1}. It is therefore necessary to postulate the formation of aggregates of peptide helices, in order to generate functional membrane channels.

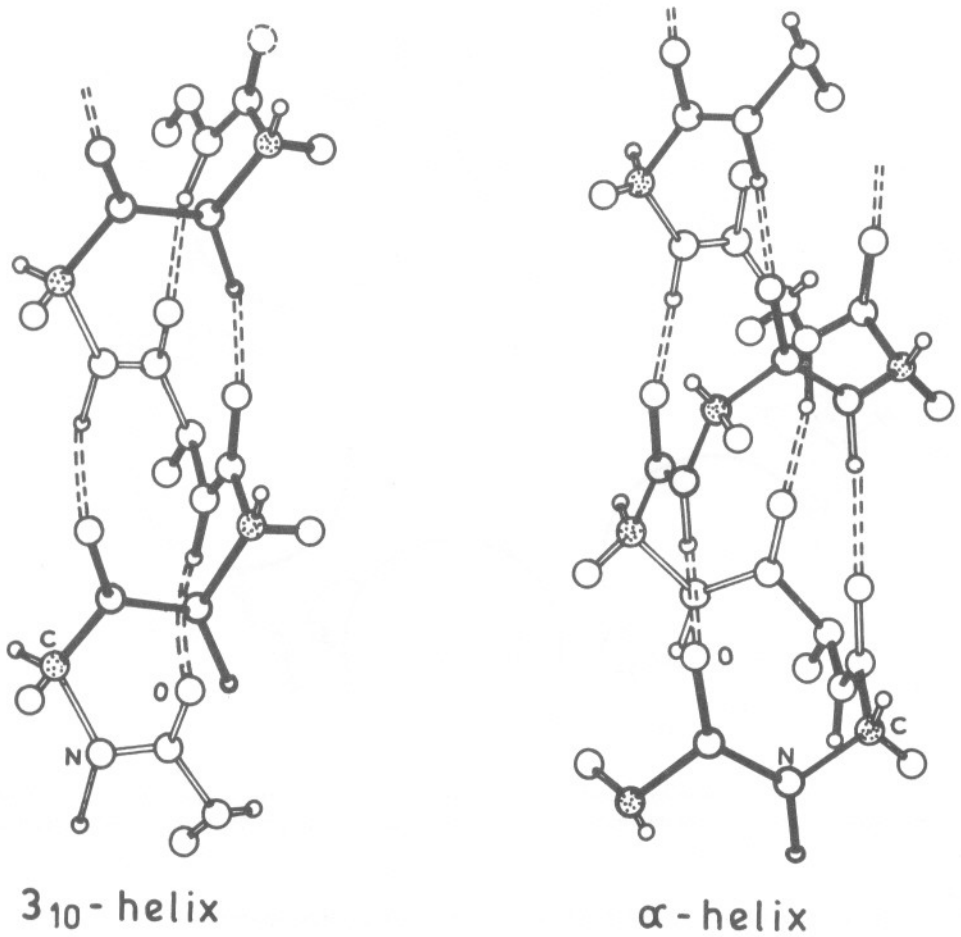

Fig. 4. Perspective view of ideal 3_{10} and α-helical structures. Note 4→1 hydrogen bonding in 3_{10} and 5→1 hydrogen bonding in α-helices.

Peptide aggregation in organic solvents

The aggregation of relatively large oligopeptide fragments of suzukacillin in organic solvents, has been examined by 270 MHz ^{1}H NMR, as a model for peptide association in the lipid phase. Both the 1–10 and 11–21 fragments of suzukacillin associate in chloroform and dimethylsulfoxide, without any alteration of monomer secondary structure (82, 83). Association is facilitated by intermolecular hydrogen bonding involving amino terminal NH groups of one molecule with carboxyl terminal CO groups of another. In the channel peptides, alamethicin, suzukacillin, trichotoxin and hypelcin, a polar Gln residue is positioned in the middle of a long stretch of hydrophobic amino acids. The side chain carboxamide group may be involved in aggregate formation by linking adjacent peptide helices by hydrogen bonding. The role of the Gln residue in promoting peptide aggregation has been established by a comparison of the concentration dependence of ^{1}H NMR parameters in the 11–21 suzukacillin fragment Boc-Gln-Aib-Leu-Aib-Gly-Leu-Aib-Pro-Val-Aib-Aib-OMe and its analog, Boc-Ala-Aib-Leu-Aib-Gly-Leu-Aib-Pro-Val-Aib-Aib-OMe, where Gln is replaced by Ala (83). Based on the approximate 3-fold symmetry of these peptide helices, the presence of a central Gln residue in the longer channel formers, the constant occurrence of a hydrogen bond interrupting Pro residue at the C-terminal end and the requirement of a suitable internal pore diameter, has resulted in the postulation of the aggregate model shown in Fig. 5 (83). This model of a cylindrical hydrophobic ag-

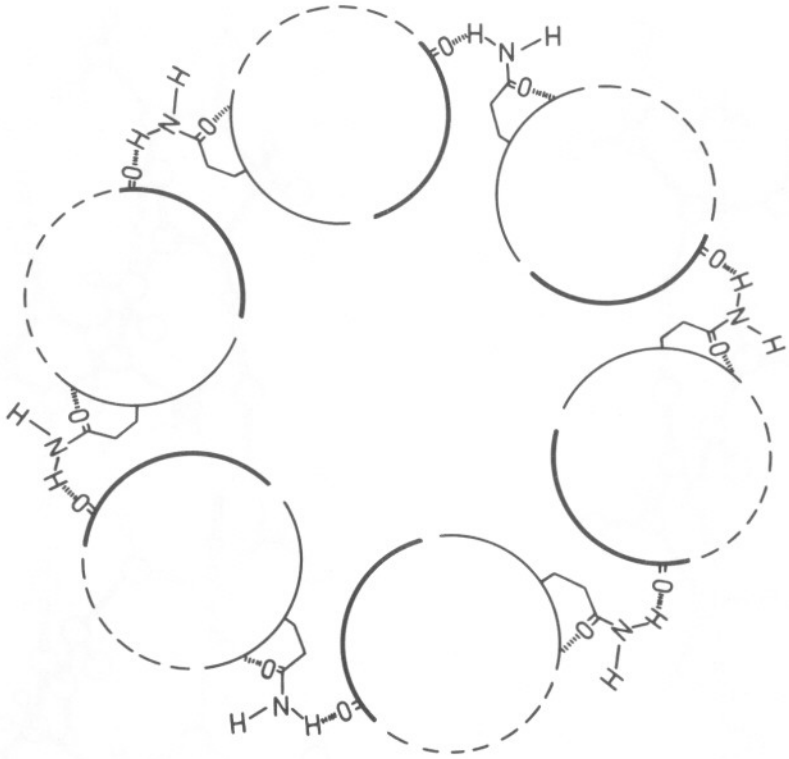

Fig. 5. Proposed model for a channel formed by alamethicin and related polypeptides. Cross section in the plane of the membrane showing the involvement of Gln side chains in intermolecular hydrogen bonding to stabilise the aggregate. Taken from ref. 83.

gregate, with a central pore can serve as a working hypothesis for rationalizing various features of the conductance behavior of alamethicin and related peptide channels.

Membrane modifying activity

Alamethicin has been shown to form voltage sensitive channels in planar, bilayer lipid membranes (BLM) (20), the ionophore-induced conductance being exponentially related to the applied voltage (84). It also induces fusion of lipid vesicles (85) and lyses erythrocytes (86) and leukocytes (87). The ionophore also renders membranes of sarcoplasmic reticulum permeable to ATP and NaF, thus unmasking ATPases (88) and adenylate cyclase (89, 90). It has been suggested that the latter activity is not related to channel forming ability, but rather solubilization of the enzyme by the amphipathic antibiotic (91). Detergent like behaviour may also be involved in its lytic activity.

Electrical measurements

Ion conduction by alamethicin has been studied by the ionophore induced electrical conductance of BLM and detection of ionophore induced transport of cations into vesicular systems. Alamethicin was among the first ionophores to be studied in a BLM set up by Mueller and Rudin (20), who obtained steady state current-voltage (I–V) curves as a function of ionic strength and ionophore concentration. Protamine sulfate induced anion selectivity in an otherwise cation selective channel. Analysis of the conductance at varying alamethicin concentrations revealed a sixth power dependence on alamethicin concentration, implying that the conducting unit may be a hexamer. Later investigations of the concentration dependence of conductance found a ninth power dependence (84, 92). While the number of monomers involved in conduction is uncertain, it is clear that an aggregate is involved. This conclusion can also be drawn on the basis of structural considerations, as the 3_{10} helical conformation like-

ly to be adopted by alamethicin is too narrow to permit the passage of ions through the helix, along its axis (83).

Steady state conductance through an ensemble of alamethicin channels is non-ohmic. Conductance is found to be exponentially related to applied voltage (84). Experiments carried out at sufficiently low antibiotic concentration and fixed membrane potential (voltage clamp) detect discrete conductance fluctuations in the temporal regime. These fluctuations have been ascribed to the formation and breakdown of individual conducting channels. Each channel displays complex conductance fluctuation behaviour ascribed to transitions among different conductance levels or states available to each individual channel during its lifetime (84, 93). Channel opening is an independent event and follows Poisson statistics, whereas conductance state transitions are best modelled as a sequential process (32, 93, 95), the pore disappearing only from its lowest conductance state.

Upto ten different conductance states have been reported (94, 96). The lowest conductance state is impermeable to Ca^{2+} and Cl^- while the higher states are permeable to Tris-H^+ and $HEPES^-$ (96). Gordon and Haydon (94) observed a cut off in conductance for $N^+(CH_3)_4$ and Tris-H^+ but this was apparently due to masking by basal KCl conductance under their experimental conditions (96). The observed transport of ATP (89, 90) argues for a very large pore diameter of some conductance states, if possible detergent-like effects (91) are shown to be absent.

The voltage-dependence of state occupancy appears to be temperature dependent. Eisenberg et al. (84), Hall (97), and Gordon and Haydon (92) observed no voltage sensitivity of the probability distributions at 20–25 °C. Boheim (98), Mueller (99), Gordon and Haydon (93), and Boheim and Kolb (32) do observe voltage sensitive transition probabilities, at lower temperatures, wherever specified, but come to different conclusions. Boheim (98) concluded that decreasing voltage increased the probability of upward transitions, while Mueller (99) came to the opposite conclusion. Part of the discrepancy could probably be ascribed to variation in the lipid composition of the membranes used (93, 99). Data in this area is fragmentary (see pages 518–523 of ref. 100). Differences observed by Baumann and Mueller (33) between membranes formed from oxidised cholesterol and glycerol diolein/diolein phosphate could probably be accounted for solely on the basis of the different voltages used with each set of membranes (100). Latorre et al (101) ascribe shifts in alamethicin I–V curves on addition of cholesterol to cholesterol-dependent changes in surface dipole potential as suggested by Szabo (102). However, Gordon and Haydon (93) found no effect of cholesterol, except when it affected membrane thickness.

From an analysis of the mean pore conductance and relaxation times, Boheim and Kolb conclude that higher pore states become more probable at higher voltages and that a formal transfer of one elementary charge across the membrane accompanies each pore state transition (32). Gordon and Haydon found that changes in applied potential can have differential effects on the transition probabilities between different levels (93). They also obtained a uniform, formal activation energy of 10 kcal $mole^{-1}$ for these transitions. (The value quoted in ref. 93 is 2 kcal $mole^{-1}$ but has been corrected in ref. 32). This has been interpreted by Boheim and Kolb (32) as representing the formation/decay of 2 hydrogen bonds in the process.

The measured voltage dependence of pore state occupancy, where reported, is inadequate to account for the observed exponential rise of conductance with applied potential. Thus, the major portion of the observed potential dependence must originate in the variation of the number of aggregates conducting at any given time. Only a small fraction of the alamethicin in the membrane participates in conduction at a particular instant. It has been estimated that when 1 oligomer is conducting, at least 10^5 molecules are adsorbed (93). On the other hand, it has recently been suggested that applied voltage could increase the number of conducting aggregates in the membrane without increasing the total membrane-phase alamethicin concentration (103).

Ion transport studies

1. Liposomes

Conceptual advances in the field of ion transport have utilized two model systems – the planar bilayer (BLM) and the bilayer vesicle (liposome). The

geometries of the two systems are complementary. Their large surface-to-volume ratios makes vesicles ideally suited for the measurement of transmembrane fluxes and spectroscopic parameters, while BLM is the system of choice for measurement of transmembrane potential and ion conductances (104). Since the sizes and geometriés of the systems of interest, viz., cells and organelles, are better approximated by liposomes than BLM, a spectroscopic assay for ion transport across liposomal membranes has been devised and correlated with BLM (105). (See Fig. 6).

Alamethicin has been shown to transport Ca^{2+}, Zn^{2+} and La^{3+} with roughly equal efficiency in liposomal systems. Synthetic fragments of alamethicin and synthetic alamethicin have been studied with this system. It was found that a minimum chain length of 13 residues is necessary for ionophorous activity; that the negative charge associated with a free carboxylic acid at or near the C terminus is inhibitory but that the charge effect decreases with increasing size, alamethicin and its benzyl ester being almost equally active; that increasing chain length and hydrophobicity of the N-terminal protecting group increased activity (106). The charge effect observed is consistent with the finding that trichotoxin methyl ester is more active in lysing erythrocytes than trichotoxin acid (47). Further, trichotoxin methyl ester, Phol-free trichotoxin and suzukacillin fragments exhibit lytic activity and voltage dependent pore formation implying that the charge and structure of the C-terminus may not be critical for activity (47, 86).

Ion transport has been detected in liposome sys-

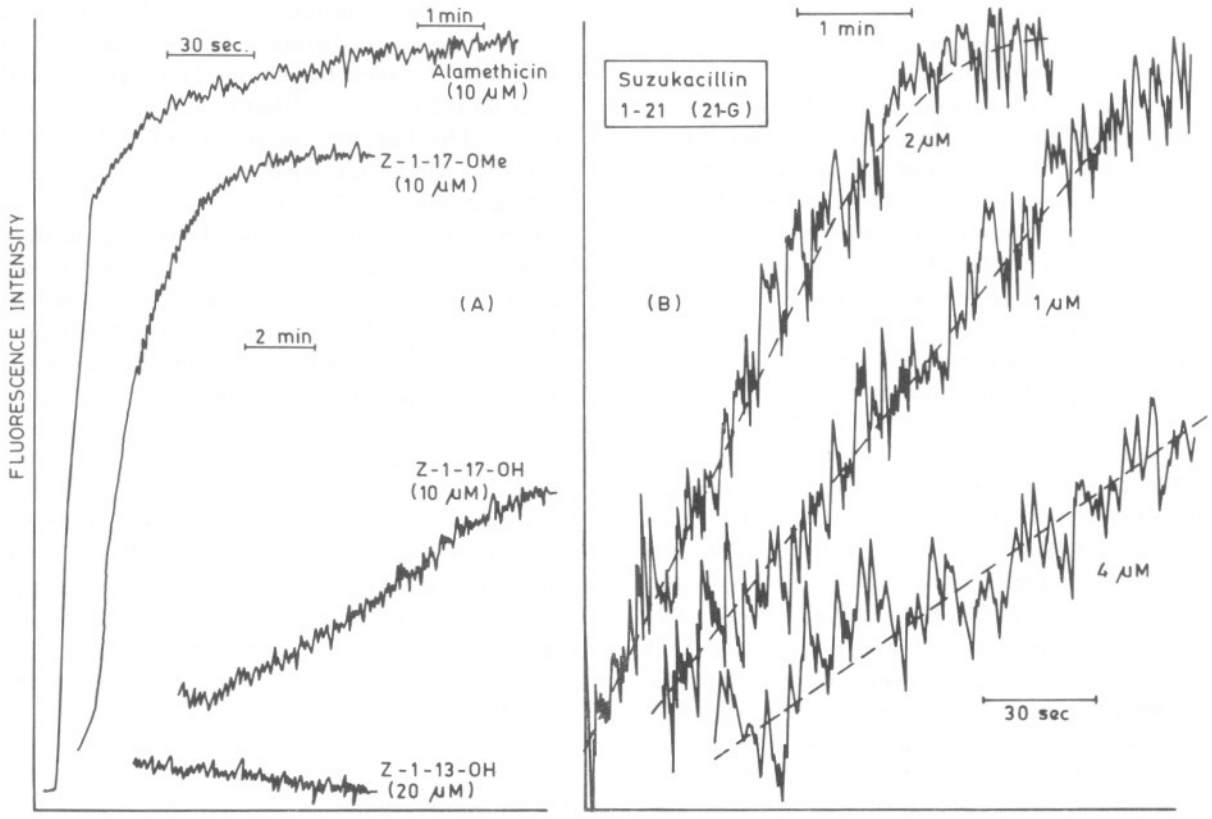

Fig. 6. Time dependent increases in CTC – Ca^{2+} fluorescence following peptide addition. Traces were started just after the addition of peptide. An increase in fluorescence is indicative of an influx of Ca^{2+} into liposomes, the initial slope of fluorescence increase being an index of ionophore efficiency. (A) Alamethicin fragments. Top two time scales for alamethicin, lower time scale for the other fragments. Z-1-17-OMe is the fragment consisting of the first 17 residues in the sequence with a benzyloxycarbonyl N-protecting group and C terminal methyl ester. Z-1-17-OH, the corresponding acid. Z-1-13-OH, the first 13 residues, N-terminal benzyloxycarbonyl, C-terminal acid. (B) Suzukacillin fragment consisting of the first 21 residues.

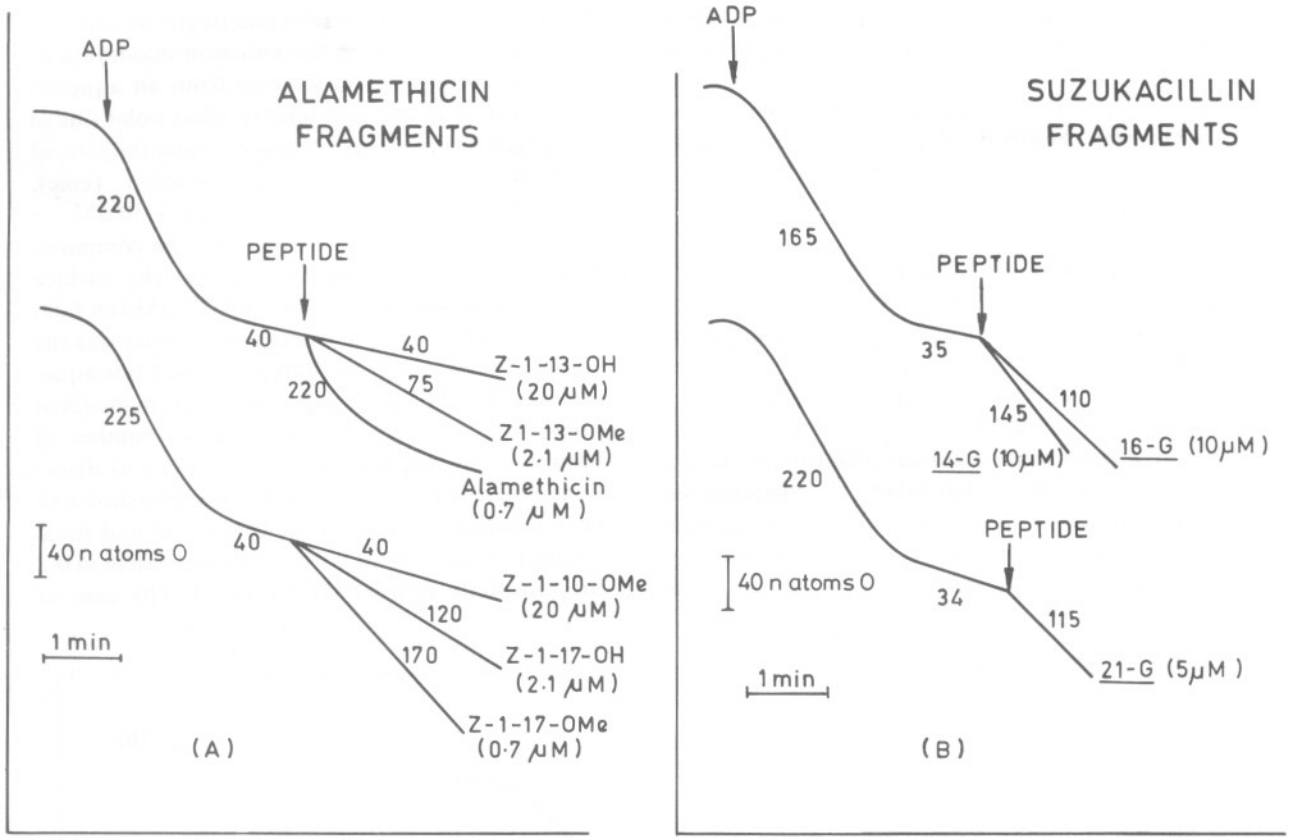

Fig. 7. Uncoupling of oxidative phosphorylation on addition of peptides. Numbers against the traces are rates of oxygen consumption in n atoms 0/ mg protein/ min. Mitochondria enter state 3 on adding ADP, whereupon oxygen is consumed to oxdise succinate, the process being coupled to the phosphorylation of ADP to ATP. On exhaustion of ADP the rate of oxygen consumption declines for lack of a substrate for phosphorylation. Addition of an uncoupler delinks the two processes leading to increased oxygen consumption. (A). alamethicin fragments – nomenclature as for Figure 6. (B). suzukacillin fragments consisting of the first 14 (14-G), 16 (16-G) and 21 (21-G) residues.

tems at concentrations such that an average of ~10 alamethicin molecules were present per vesicle. Under such conditions transport into nearly all liposomes was detected implying that a large excess of inactive monomers is not necessary for conduction.

2. Uncoupling of oxidative phosphorylation

The coupling of oxidation and phosphorylation in mitochondria requires the cyclic transport of protons (107, 108). A combination of valinomycin and nigericin can delink the two processes (109). It has been proposed that uncouplers, like the ionophoric combination, mediate coupled cyclical cation transport, thereby replacing one coupled process with another (110). A population of non-rectifying channels should permit passage of cations, either way across the mitochondrial membrane and so should function as uncouplers. Alamethicin and the hypelcins have been shown to uncouple oxidative phosphorylation, in rat liver mitochondria (111). The efficiency of various synthetic fragments in ion translocation has been investigated by comparing their efficiencies as uncouplers (112) (Fig. 7). The results obtained paralleled those with the liposomal assay leading to the following conclusions:

1. A minimum length of 13 residues is required for ion translocation.
2. Longer peptides are more active than short ones.
3. Negative charge on the peptide is inhibitory. The inhibitory effect decreases with increasing chain length.

4. Bulky, non-polar N-protecting groups enhance activity. This effect is also less pronounced in longer peptides.

It was, therefore, concluded that the same process underlies the critical step in both assays – probably the formation of functional channels.

Peptide aggregation in aqueous solution

The concentration dependence of alamethicin induced conductance establishes that the functional channel is an aggregate of peptide monomers. The factors which favour the formation of active channels – hydrophobicity and neutralization of charge repulsions – are those that favour the aggregation of the peptides in aqueous solution. Aggregation has been studied using peptides fluorescently labelled with the dansyl group at the N-terminus, a modification which does not inactivate the peptides (113, 114). The shift in the emission maximum of the fluorophore in transferring from an aqueous environment in the monomer to a less polar one in an aggregate (115) was used to estimate the critical aggregation/micellization concentration (cmc), which was found to be in the range of 3–30 μM for the peptide esters (Fig. 8). and may be compared with the reported values of 2.4 μM (by surface tension measurements) (116) and 2.5 μM (by CD) (80) for alamethicin. The decapeptide ester was the smallest in this series to aggregate in salt free aqueous solution. The acids aggregated only in media of high ionic strength. The aggregation number of natural alamethicin in aqueous solution, as determined by sedimentation studies, has been shown to be a function of peptide concentration and ionic strength, being ~16 at 0.6% w/v alamethicin in 0.2 M phosphate buffer, pH 8.0 (116). The ease of

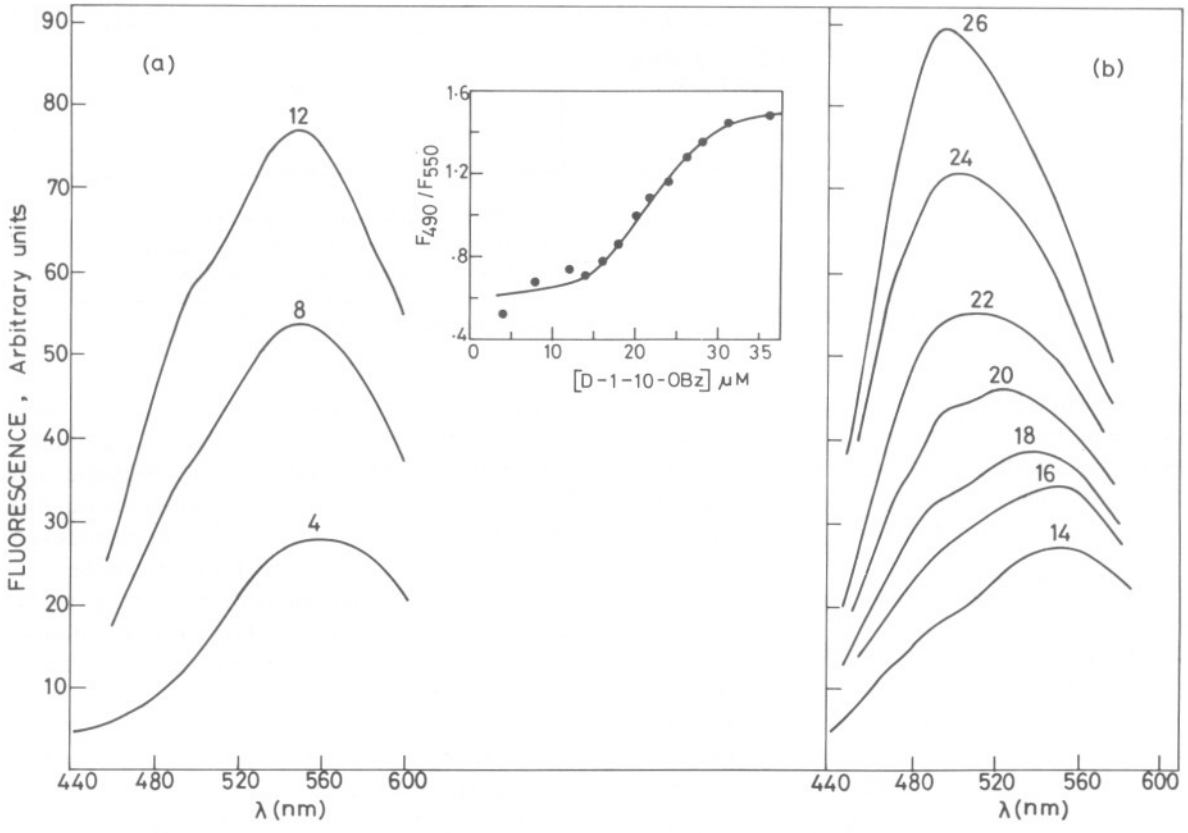

Fig. 8. Emission spectra (λ_{ex} = 333 nm) of D-1-10-OBz, a fragment of alamethicin consisting of the first 10 residues with dansylglycyl at the N-terminus and benzyl ester at the C-terminus as a function of concentration, in μM which is indicated against the traces. The ratio of intensities at 490 and 550 nm. F_{490}/F_{550} is plotted as an inset to the figure.

aggregation for the peptides follows the same sequence as for functional activity indicating that aqueous phase aggregation may be a crucial step in the formation of transmembrane channels (114).

The large decrease in formal activation energy for pore state transitions at high temperatures has been explained by a reduced tendency of the monomers to aggregate, implying an enthalpically favored aggregation process (32). A ΔH for aggregation of -1 to -3 kcal mole^{-1} has been found, being less negative for longer peptides (114). This is expected as hydrophobic interactions should increase for the longer peptides and these interactions are entropically driven with $\Delta H = 0$ or slightly positive (117, 118). Hysteresis is observed in the aggregation-disaggregation process. Disaggregation occurs on a much slower time scale than aggregation – the former being in the range of hours while the latter is complete in under a second. Relaxation from an aggregated state in response to dilution does not follow first order kinetics (114). Cooperativity is observed in the aggregation process (114) and in the formation of alamethicin (80, 92) and other channels (119). Treatment of two-dimensional cooperativity by the Ising model predicts metastable states and consequent hysteresis effects for sub-critical values of the cooperativity parameter (120).

The observation of functional activity by both assay procedures below the measured cmc (114) can be ascribed to the high ionic strength prevailing in the Stern layer of ionic micelles and membrane surfaces, which is estimated to be in the region of 1–3 M (121). The peptide cmc values decrease with increasing ionic strength and a log–log relationship for the two parameters is observed (114), analogous to that observed for detergent micelles (122). Thus, in 3 M NaCl, the cmc values of the longer peptides are too low to measure (114).

Models of the channel

Models proposed to account for the conductance characteristics of the alamethicin channel envisage the aggregation of peptide molecules to form an aqueous core, which may then take up discrete conductance states by undergoing changes in either aggregation number (32), or positional/conformational changes of the monomer (93, 97). Kinetic data have been interpreted in terms of either model. Evidence in favor of the first model comes from the fact that the various conductance states have different cross-sectional areas as judged by a sieving method. The lowest conductance state is impermeable to Ca^{2+} and Cl^- (96), whereas the higher levels are permeable to Tris-H^+ and $HEPES^-$ (96) and, probably, ATP (88–91). Further, a formal movement of one electronic charge is associated with each pore state transition, which has an activation energy corresponding to 2 hydrogen bonds formed/broken in the process (32). Also, freezing of the membrane lipid eliminates conductance fluctuations (123) indicating that lateral mobility may be required for this process. On the other hand, Gordon and Haydon (93) report that changes in applied voltage do not affect all transition probabilities in the same way, as would be expected if the only effect of applied voltage had been to increase the number of monomers in the membrane phase.

Fleischmann et al. (95), analysing conductance fluctuations without biasing their data to single channel events, concluded that the system is Markovian, except for the lowest conductance level. Transitions occur mainly between adjacent conductance states and the probability of such a transition is dependent on the state of current occupancy and is independent of the previous history of the pore. This confirms the assumptions made by Boheim and Kolb (32) regarding the adoption of conductance states in consecutive order. Fleischman et al. also propose a model in which pore state changes involve alterations in the size of the pore lumen though they envisage a system of fused pores with common elliptical edges (95).

One of the major pieces of evidence in favor of the "barrel-stave" hypothesis of Boheim and Kolb (32) is the correlation of cross-sectional area of the channel with conductance (96). The basis for considering large, solvent containing pores with a specific conductivity equal to bulk solvent, at least for the higher conductance states, is that ion selectivity sequences for alkali cations follow the same order as their mobilities in water. Further, single channel conductances of all levels are proportional to the conductance of the bulk solution (84). However, attempts to correlate cross-sectional area with conductance (96) ignore the area occupied by the rod-like monomers and thus overestimate the channel diameter. The fortuitous agreement obtained with experimental results (96) is indicative of either field

perturbations or alteration of the medium within the channel, or both. Also, channel diameter is not the sole determinant of channel conductance. Amphotericin B, with a conductance 1/40 that of gramicidin (13, 124), has twice the diameter (125, 14).

It would be fruitful at this stage to enumerate the basic data that must be incorporated in or explained by any comprehensive molecular model of the alamethicin channel. These are:

1. The pore consists of an aggregate (20, 84, 92, 94) of rod-like helices (46, 83). The number of monomers involved in aqueous phase aggregates is variable and depends on both the concentration of peptide and ionic strength of the medium (116).
2. Fluctuations between various conductance states, as observed in single channel experiments, must have relatively low activation energies (1–10 kcal mole^{-1}), so as to be facile (93).
3. Not all pores need have the same cross-sectional area for conduction, in keeping with sieving experiments (96).
4. Macroscopic conductance is non-ohmic (positive deviations being observed) (84, 126). This requires a channel structure with features that allow for a strong interaction with an applied electric field.

It may be noted that quantitative agreement with kinetic data is, at present, an unrealistic goal as this requires suitable modelling of peptide–lipid interactions. The composition of the membrane is known to strongly influence the observed channel characteristics (100, 127). Very few studies have focussed on alamethicin-lipid interactions (85, 128). Moreover, nearly all published single channel data utilize natural alamethicin which has been shown to consist of at least 12 different species (52), the two major fractions of which differ in their conductance characteristics (126). In this connection, it is interesting to note that the complex mixture of polypeptides making up the bacterial extract exhibits much sharper probability histograms for pore state occupancy than a synthetic peptide with analogous activity (129).

Helix dipole model

The alamethicin monomer is likely to take up a helical structure (3_{10} or α) which is too narrow to allow the passage of ions as large as Na^+ through the helix interior. A feature of such a structure is the presence of a large dipole moment arising from the near-parallel orientation of the dipoles of the peptide units making up the helix (130). Recently, much interest has been generated in the area of protein structure, with helix dipoles being shown to be a major stabilizing force along with hydrogen bonding, hydrophobic and electrostatic interactions (131). In the case of an α-helix, the resultant macro-dipole moment is estimated to be 3.5 D per 1.5 Å of the helix length (132). For a 3_{10} helix, the peptide dipoles are slightly inclined to the helix axis, but the greater length of the 3_{10} helix (for an equal number of residues) would result in similar values for the net dipole moment. The reported dipole moment of natural alamethicin is consistent with this estimate, being 67 D (133). It has previously been recognized that the dipole moment of alamethicin may have a role to play in its function (32, 92, 98, 133, 134). The generation of voltage dependent membrane structures using dipoles has also been treated (135). However, it has not been realized that the major component of the alamethicin dipole moment arises from the helix dipole or that this macro-dipole could perturb the field within the channel. The dipole induced field within an α-helix has been shown to be adequate to account for the unidirectional transport of protons (81) and, in the case of high net dipole states (Fig. 9) would perturb the local potentials. Transitions between states of differing net dipole moment for a particular aggregate (n-mer) or between low-dipole states of an n-mer and an $(n \pm 1)$-mer could give rise to the observed 'charge translocation' events (32). However, the voltage dependence of these transitions would be manifest mainly at low temperatures, since the difference in energies between the parallel and antiparallel orientations of a helix of dipole moment 65 D is only 4.5×10^{-14} ergs molecule^{-1} (0.668 kcal mole^{-1}) at 300 °K. Again, the high dipole states of aqueous phase aggregates, are disfavored due to dipole–dipole interactions. For example, the difference in energies of the zero and two-dipole states (Fig. 9), as estimated according to Hol et al. (131) is 61 kcal mole^{-1}, in the absence of an applied potential. Thus, the 'pre-aggregate' existing in the aqueous phase has to be in a low dipole state, preferably a 'minimum dipole' state. However, a field of 2×10^5 V cm^{-1} acting on the peptides

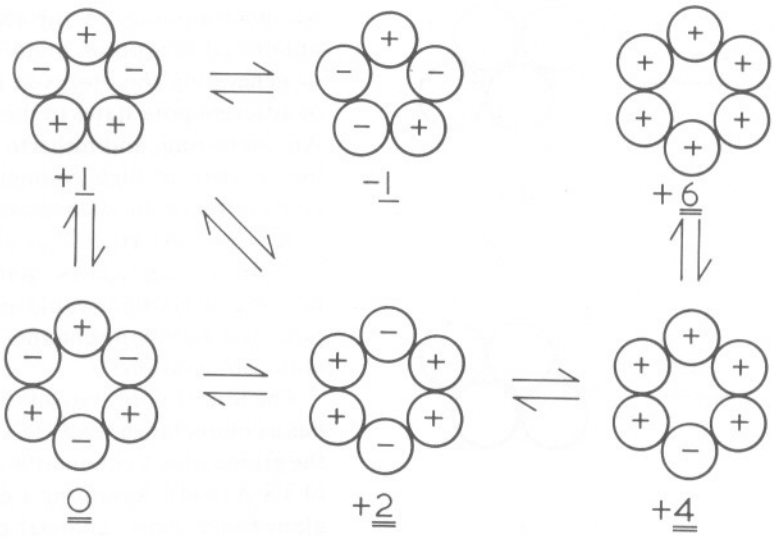

Fig. 9. Schematic cross-sectional views of polypeptide channels. + and – indicate opposite orientations of the helices. Numbers below the figures indicate net dipole moment in arbitrary units. The equilibria indicated are schematic and do not imply pathways. For instance, the transition of 0 to +2 may involve +1 as an intermediate. Note that changes in pore state could involve changes in both dipole moment and channel diameter.

once in the membrane phase could favor the formation of aggregates with a net dipole moment. Analogs of trichotoxin and suzukacillin modified at the C terminus have been reported to form voltage sensitive channels indicating that the charge and structure of the C terminus are not critical for voltage sensitivity (47, 86). Hence, neither the 'charge translocation event' detected during pore state transitions (32), nor the proposed effect of voltage in increasing the population of conducting channels (32) can be ascribed to the charge on the C terminus but, instead, must be due to reorientation of the helix dipole.

Both aqueous phase (32) and membrane phase (136, 137) aggregation of alamethicin monomers has been proposed. Studies of the transport of suzukacillin and alamethicin across lipid membranes, establishes that channel formation enhances the rate of monomer exchange between the two surfaces (138). The excellent correlation of the ease of aggregation of synthetic alamethicin fragments with their functional activity (114) implicates the formation of aqueous phase aggregates, which then insert into the membrane. The voltage dependence of macroscopic conductance is ascribed mainly to an increase in the number of conducting aggregates in the membrane in response to an applied field. Models to account for this imply 'high dipole' pre-aggregates pushed into the membrane by the applied potential (32, 33). Since the pre-aggregates are likely to be 'low dipole' entities, this scheme may require modification. Boheim and Kolb (32) envisage the initial entry of 2 or 3 monomers of a hexameric pre-aggregate, in response to an applied potential. These could be helices in the preaggregate with suitably oriented dipoles. Insertion of the remaining helices into the membrane against the electric field would be stabilized by the formation of a low dipole aggragate in the membrane. It should be noted that an applied potential is not obligatory for the entry of alamethicin into lipid membranes (103, 139). Indeed, a peptide as hydrophobic as alamethicin is likely to partition preferentially into the lipid phase. Microconductance fluctuations could then occur either by interchange of monomers among adjacent n-mers thereby changing the net dipole moment and dipole induced field within the channel; or by monomer-aggregate equilibrium which would change the area of the conducting pore in addition to field alterations (Fig. 9). Figure 10 shows how rearrangement of the helices could result in a 'closed pore' analogous to the model proposed for gap junctions (2). While lateral mobility of monomers is required for all these processes,

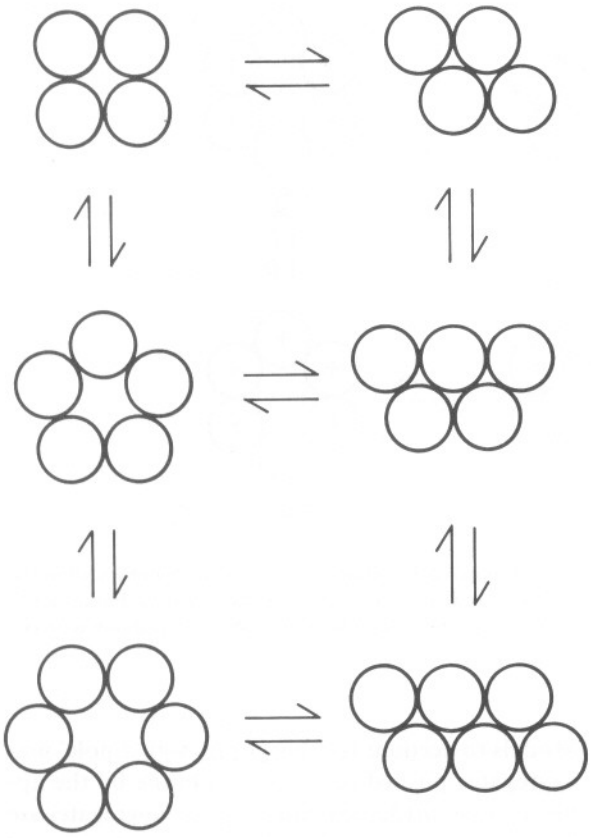

Fig. 10. Schematic models of pore opening and closing by suitable rearrangement of peptide helices, analogous to the open and closed states proposed for gap junctions.

and is obligatory for pore state fluctuations (123) the transition probabilities also depend on the extent to which the applied potential stabilizes the non-zero net dipole states. Thus, preferential stabilization of non-zero net dipole states by applied potential will be superimposed on the effect of increasing the number of ionophore molecules in the membrane, so generating the observed non-uniform response of different pore states to the applied potential (93). An interesting, and hitherto unexplained observation is that, at high enough field strengths, measured pore conductivity exceeds the conductivity of bulk water (93). High field strengths could stabilize high-dipole aggregates and the dipole induced fields so generated would perturb the membrane potential within the channel, leading to this anomalous observation.

The lowest pore state of the alamethicin channel has a conductance ~20% less than that reported for the gramicidin A channel (96), which has a diameter of 3.8 Å (140). Assuming a diameter of 5 Å for the alamethicin helix, channel diameters can be estimated for symmetric arrangements of monomeric helices around a central aqueous core. The pentamer, with an estimated channel diameter of 3.5 Å would then form the lowest conducting state, the tetramer with a diameter of 2.1 Å being non-conducting. Table 1 lists some known pore formers and their estimated channel diameters for comparison. Gateability phenomena have been recently modelled on the bases of non-conducting monomers aggregating spontaneously to form non-conducting aggregates, which undergo a voltage induced transition to a conducting state (141).

A feature of the proposed model for the alamethicin channel is that it consists of an aggregate of helices arranged such that only apolar residues face the interior of the channel – thus forming a 'hydrophobic channel'. This is in contrast to the gramicidin channel, which is lined by suitably positioned and oriented carbonyls providing binding sites for

Table 1.

Channel	Diameter Å	Method used	Channel	Diameter Å	Method used
Gramicidin A (140)	3.8	X-ray	K^+ channel of nerve (160)	3	Sieving
Amphotericin B (14)	8	Sieving	Gap junctions (mammalian) (161)	16–20	Sieving
			(insect) (161)	20–30	Sieving
Diphteria toxin (156)	8	Conductance	*E. coli* pores 1a, 1b, 1c (162)	12–14	Conductance
(157)	18	Sieving			
Porin form *E. coli* (158)	9	Conductance	λ receptor (163)	15	Conductance
Na^+ channel of nerve (159)	3 × 5	Sieving	*Salmonella typhimurium* (164) pores	14	Conductance
Nystatin (14)	8	Sieving	*Ps aeruginosa* protein F (162)	22	Conductance

the ions passing through it (140, 142). The dissolution of apolar molecules in water is known to alter the structure of water in the immediate vicinity of the solvent (143). Thus, the narrow cylinders of water, a few molecules across, present in the channel interior, are likely to have properties quite distinct from bulk solvent. Few attempts have been made to model these aqueous channels but it has been suggested that alterations in the structure of the water may result in ion selectivity for the channel (144). Conversely, ion solvent interactions may determine conductance characteristics. It is interesting to note that gating of muscle K^+ channel, depends on the permeating ion species (145). Also, the interaction of toxins with the sodium channel is known to alter the ion selectivity of the channel (146). Further, such an array of structured water may serve as a very efficient proton translocation system, as in ice (144, 147, 148). The high efficiency of these channels as uncouplers of oxidative phosphorylation may support this contention (112).

Conclusions

The channel model described above ascribes a largely structural role for the cylindrical peptide aggregate in stabilizing aqueous bridges across lipid bilayers. The high H^+ permeability observed for unmodified lipid bilayers (149, 150) suggests that narrow aqueous columns do, in fact, span the membrane. Aib containing peptide channels serve as a scaffolding for supporting larger aqueous columns, which serve to enhance ion permeabilities of lipid bilayers. The selectivity of these channels may be modulated by alterations in aggregate size and precise modes of aggregation, which in turn alter the structures of the aqueous matrix. Direct interaction of ions with alamethicin and related peptides is unlikely to be of functional significance, in marked contrast to ionophores like valinomycin of gramicidin A (140, 142). Recent crystal structure analyses of antamanide (151) and an Aib pentapeptide (152) provide models for the formation of hydrophobic channels in the solid state.

The proposed structural model for the Aib peptide channels has considered a largely helical conformation for the peptide monomer in the lipid phase. While these structures are stabilized by the occurrence of Aib residues, similar helical conformations have been proposed as important structural determinants for protein segments during transit through membranes (153). Association of peptide helices in membranes is also exemplified in the structure of bacteriorhodopsin (154).

The membrane channel model postulated in this review is intended to stimulate further experimental approaches to the study of the molecular mechanisms involved in determining the ionophoric activity of alamethicin and related polypeptides. Since the cylindrical pores are postulated to be stabilized both by dipole–dipole interactions and hydrogen bonding involving the central Gln residue, the model is amenable to experimental verification. Alteration of the charge of the peptide by esterification or amidation of the terminal Glu residue should modify the single channel characteristics but conductance of the channel aggregates should still be voltage sensitive. Deamidation of the central Gln residue should destabilize the channel both by eliminating the possibility of intermolecular hydrogen bonding and by introducing electrostatic repulsions between monomers, leading to significantly shorter lifetimes. Substitution of an apolar residue for Gln affects only the hydrogen bonding capability and the effect on channel lifetime should be less pronounced than deamidation. Further, the precise sequence of residues is not expected to be critical for the formation of channels as long as the peptide is long enough (15–20 residues), is constrained to adopt either α or 3_{10} helical structures, composed mainly of apolar residues and capable of forming intermolecular hydrogen bonds near the centre of the helix so as to stabilize the channel aggregate. Preliminary reports of the conductance behaviour of Aib containing channel analogs are consistent with these predictions (155).

Acknowledgements

Research in this laboratory in the area of membrane active peptides has been supported by the Department of Science and Technology, Government of India. PB is the recipient of a Career Award from the University Grants Commission. MKM thanks the Indian Council of Medical Research for a fellowship.

References

1. Giebisch, G., Tosteson, D. C. and Ussing, H. H., 1978. Membrane Transport in Biology, Vol. 1, Springer-Verlag, Berlin.
2. Loewenstein, W. R., 1981. Physiol. Rev. 61: 829–913.
3. Shamoo, A. E. and Murphy, T. J., 1979. Current Topics in Bioenergetics (Sanadi, D. R., ed.) Vol. 9: 147–177, Academic Press, New York.
4. Montal, M., Darszon, A. and Schindler, H., 1981. Quart. Rev. Biophys. 14: 1–79.
5. Pressman, B. C., 1976. Ann. Rev. Biochem. 45: 501–530.
6. Ovchinnikov, Yu. A., Ivanov, V. T. and Shkrob, A. M., 1974. Membrane Active Complexones, Elsevier, Amsterdam.
7. Ovchinnikov, Yu. A. and Ivanov, V. T., 1975. Tetrahedron 31: 2177–2209.
8. Hamilton, J. A., Sabesan, M. N. and Steinrauf, L. K., 1981. J. Am. Chem. Soc. 103: 5880–5885.
9. Mueller, P., 1976. in Horizons in Biochemistry and Biophysics (Quagliariello, E., Palmieri, F. and Singer, T. P., eds.) Vol. 2, pp. 230–284, Addison-Wesley, Reading.
10. Fambrough, D. M., 1979. Physiol. Rev. 59: 165–227.
11. Urry, D. W., 1977. Int. J. Quantum Chem. Quantum Biol. Symp. 4: 25–42.
12. Latorre, R. and Alvarez, O., 1981. Physiol. Rev. 61: 77–150.
13. Hladky, S. B. and Haydon, D. A., 1972. Biochim. Biophys. Acta 274: 294–312.
14. Holz, R. W. and Finkelstein, A., 1970. J. Gen. Physiol. 56: 125–145.
15. Cass, A., Finkelstein, A. and Krespi, V., 1970. J. Gen. Physiol. 56: 100–124.
16. Alvarez, O., Diaz, E. and Latorre, R., 1975. Biochim. Biophys. Acta 389: 444–448.
17. Bean, R. C., Shepherd, W. C. and Eichner, J., 1969. J. Gen. Physiol. 53: 741–757.
18. Muller, R. and Finkelstein, A., 1972. J. Gen. Physiol. 60: 263–284.
19. Ramakrishnan, V., Darszon, A., Phillips, M. C. and Montal, M., 1980. Ann. N.Y. Acad. Sci. 358: 36–42.
20. Mueller, P. and Rudin, D. O., 1968. Nature 217: 713–719.
21. Boheim, G., Janko, K., Leibfritz, D., Ooka, T., Konig, W. A. and Jung, G., 1976. Biochim. Biophys. Acta 433: 182–199.
22. Urry, D. W., 1971. Proc. Natl. Acad. Sci. (USA), 68: 672–676.
23. Bamberg, E., Appell, H.-J. and Alpes, H., 1977. Proc. Natl. Acad. Sci. (USA) 74: 2402–2406.
24. Bradley, R. J., Prasad, K. U. and Urry, D. W., 1981. Biochim. Biophys. Acta 649: 281–285.
25. Finkelstein, A. and Andersen, O. S., 1981. J. Membr. Biol. 59: 155–171.
26. Enos, B., Eisenman, G., Hägglund, J. and Sandblom, J., 1980. Fed. Proc. 39: 1655.
27. Neher, E., 1975. Biochim. Biophys. Acta 401: 540–544.
28. Eisenman, G., Sandblom, J. and Neher, E., 1978. Biophys. J. 22: 307–340.
29. Eisenman, G., Enos, B., Hägglund, J. and Sandblom, J., 1980. Ann. N.Y. Acad. Sci. 339: 8–20.
30. Busath, D. and Szabo, G., 1981. Nature 294: 371–373.
31. Latorre, R., Ehrenstein, G. and Lecar, H., 1972. J. Gen. Physiol. 60: 72–85.
32. Boheim, G. and Kolb, H.-H., 1978. J. Membr. Biol. 38: 99–150.
33. Baumann, G. and Mueller, P., 1974. J. Supramol. Str. 2,: 538–562.
34. Lecar, H., Ehrenstein, G. and Latorre, R., 1975. Ann. N.Y. Acad. Sci. 264: 304–326.
35. Holz, R. W., 1974. Ann. N.Y. Acad. Sci. 235: 469–476.
36. Andreoli, T. E., 1974. Ann. N.Y. Acad. Sci. 235: 448–454.
37. Hamill, O. P. and Sakmann, B., 1981. Nature 294: 462–464.
38. Gration, K. A. F., Lambert, J. J., Ramsey, R. L., Rand, R. P. and Usherwood, P. N. R., 1982. Nature 295: 599–601.
39. Jung, G., Konig, W. A., Leibfritz, D., Ooka, T., Janko, K. and Boheim, G., 1976. Biochem. Biophys. Acta 433: 164–181.
40. Pandey, R. C., Carter Cook, J., Jr., and Rinehart, K. L., Jr., 1977. J. Am. Chem. Soc. 99: 8469–8483.
41. Pandey, R. C., Meng, H., Carter Cook, J., Jr. and Rinehart, K. L., Jr., 1977. J. Am. Chem. Soc. 99: 5203–5202.
42. Pandey, R. C., Carter Cook, J., Jr. and Rinehart, K. L., Jr., 1977. J. Am. Chem. Soc. 99: 5205–5206.
43. Bruckner, H., Konig, W. A., Greiner, M. and Jung, G., 1979. Angew. Chem. Int. Ed. Engl. 18: 476–477.
44. Fujita, T., Takaishi, Y. and Shimomoto, T., 1979. J. Chem. soc. Chem. Commun. 413–414.
45. Rinehart, K. L., Jr., Gaudioso, L. A., Moore, M. L., Pandey, R. C., Carter Cook, J., Jr., Barber, M., Sedgwick, R. D., Bordoli, R. S., Tyler, A. N. and Green, B. N., 1981. J. Am. Chem. Soc. 103: 6517–6520.
46. Nagaraj, R. and Balaram, P., 1981. Acc. Chem. Res. 14: 356–362.
47. Boheim, G., Irmscher, G. and Jung, G., 1978. Biochim. Biophys. Acta 507: 485–506.
48. Meyer, C. E. and Reusser, F., 1967. Experientia 23: 85–86.
49. Ovchinnikov, Yu. A., Kiryushkin, A. A. and Kozhevnikova, I. V., 1971. Gen. Chem. USSR 41: 2105–2116.
50. Payne, J. W., Jakes, R. and Hartley, B. S., 1970. Biochem. J. 117: 757–766.
51. Martin, D. R. and Williams, R. J. P., 1976. Biochem. J. 153, 181–190.
52. Balasubramanian, T. M., Kendrick, N. C. E., Taylor, M., Marshall, G. R., Hall, J. E., Vodyanoy, I. and Reusser, F., 1981. J. Am. Chem. Soc. 103: 6127–6132.
53. Gisin, B. F., Davis, D. G., Borowska, Z. K., Hall, J. E. and Kobayashi, S., 1981. J. Am. Chem. Soc. 103: 6373–6377.
54. Ramachandran, G. N. and Sasisekharan, V., 1968. Adv. Prot. Chem. 23: 283–438.
55. Marshall, G. R. and Bosshard, H. E., 1972. Circ. Res. Suppl. 30–31, 143–150.
56. Prasad, B. V. V. and Sasisekharan, V., 1979. Macromolecules 12: 1107–1110.
57. Burgess, A. W. and Leach, S. J., 1973. Biopolymers 12: 2599–2605.
58. Shamala, N., Nagaraj, R. and Balaram, P., 1977. Biochem. Biophys. Res. Commun. 79: 292–298.
59. Shamala, N., Nagaraj, R. and Balaram, P., 1978. J. Chem. Soc. Chem. Commun. 996–997.

60. Prasad, B. V. V., Shamala, N., Nagaraj, R., Chandrasekaran, R. and Balaram, P., 1979. Biopolymers 18: 1635–1646.
61. Prasad, B. V. V., Shamala, N., Nagaraj, R. and Balaram, P., 1980. Acta Crystallogr. B36: 107–110.
62. Venkatachalapathi, Y. V., Nair, C. M. K., Vijayan, M. and Balaram, P., 1981. Biopolymers 20: 1123–1136.
63. Benedetti, E., Pedone, C. and Toniolog, C., 1981. Peptides 1980. (Brunfeldt, K. ed.) pp. 619–624, Scriptor, Copenhagen.
64. Smith, G. D., Pletnev, V. Z., Duax, W. L., Balasubramanian, T. M., Bosshard, H. E., Czerwinski, E. W., Kendrick, N. E., Mathews, F. S. and Marshall, G. R., 1981. J. Am. Chem. Soc. 103: 1493–1501.
65. Aubry, A., Protas, J., Boussard, G., Marraud, M. and Neel, J., 1978. Biopolymers 17: 69–89.
66. Prasad, B. V. V., Ravi, A. and Balaram, P., 1981. Biochem. Biophys. Res. Commun. 103: 1138–1144.
67. Prasad, B. V. V., Balaram, H. and Balaram, P., 1982. Biopolymers 21: 1261–1273.
68. Francis, A. K., Iqbal, M., Balaram, P. and Vijayan, M., 1982. J. Chem. Soc., (in press).
69. Donohue, J., 1953. Proc. Natl. Acad. Sci. (U.S.A.) 39: 470–478.
70. Pauling, L. and Corey, R. B., 1951. Proc. Natl. Acad. Sci. (U.S.A.) 37: 272–275.
71. Butters, T., Hutter, P., Jung, G., Pauls, N., Schmitt, H., Sheldrick, G. M. and Winter, W., 1981. Angew. Chem. Int. Ed. Engl. 20, 889–890.
72. Nagaraj, R., Shamala, N. and Balaram, P., 1979. J. Am. Chem. Soc. 101: 16–20.
73. Nagaraj, R. and Balaram, P., 1981. Biochemistry 20: 2828–2835.
74. Iqbal, M. and Balaram, P., 1981. J. Am. Chem. Soc. 103: 5548–5552.
75. Iqbal, M. and Balaram, P., 1981. Biochemistry 20: 4866–4871.
76. Venkatachalapathi, Y. V. and Balaram, P., 1981. Biopolymers 1137–1142.
77. Pulla Rao, Ch., Nagaraj, R., Rao, C. N. R. and Balaram, P., 1979. FEBS Lett. 100: 244–248.
78. Pulla Rao, Ch., Nagaraj, R., Rao, C. N. R. and Balaram, P., 1980. Biochemistry 19: 425–431.
79. Mayr, W., Oekonumopulos and Jung, G., 1979. Biopolymers 18: 425–450.
80. Jung, G., Dubischar, N. and Leibfritz, D., 1975. Eur. J. Biochem. 54: 395–409.
81. Van Duijnen, P. Th. and Thole, B. T., 1981. Chem. Phys. Lett. 83: 129–133.
82. Iqbal, M. and Balaram, P., 1982. Biopolymers 21: 1427–1433.
83. Iqbal, M. and Balaram, P., 1981. Biochemistry, 20: 7278–7284.
84. Eisenberg, M., Hall, J. E. and Mead, C. A., 1973. J. Membr. Biol. 14: 143–176.
85. Lau, A. L. Y. and Chan, S. I., 1974. Biochemistry 13: 4942–4948.
86. Irmscher, G. and Jung, G., 1977. Eur. J. Biochem. 80: 165–174.
87. Bessler, W. G., Ottenbreit, B., Irmscher, G. and Jung, G., 1979. Biochem. Biophys. Res. Commun. 87: 99–105.
88. Jones, L. R., Besch, H. R., Jr. and Watanabe, A. M., 1977. J. Biol. Chem. 252: 3315–3323.
89. Besch, H. R., Jr., Jones, L. R., Fleming, J. W. and Watanabe, A. M., 1977. J. Biol. Chem. 252: 7905–7908.
90. Jones, L. R., Maddock, S. W. and Besch, H. R., Jr., 1980. J. Biol. Chem. 255: 9971–9980.
91. Bonnafous, J.-C., Dornand, J. and Mani, J.-C., 1979. Biochem. Biophys. Res. Comm. 86: 536–544.
92. Gordon, L. G. M. and Haydon, D. A., 1972. Biochim. Biophys. Acta 255: 1014–1018.
93. Gordon, L. G. M. and Haydon, D. A., 1976. Biochim. Biophys. Acta 436: 541–556.
94. Gordon, L. G. M. and Haydon, D. A., 1975. Phil. Trans. Roy. Soc., London, Ser. B 270: 433–447.
95. Fleischmann, M., Gabrielli, C., Labram, M. T. G., Mc Mullen, A. I. and Wilmshurst, T. H., 1980. J. Membr. Biol. 55: 9–27.
96. Hanke, W. and Boheim, G., 1980. Biochim. Biophys. Acta 596: 456–462.
97. Hall, J. E., 1975. Biophys. J. 15: 934–937.
98. Boheim, G., 1974. J. Membr. Biol. 19: 277–303.
99. Mueller, P., 1975. In MTP Reviews of Science. Biochemistry Series I (Racker, E. ed.) Vol. 1, pp. 265–280, Butterworths, London.
100. Hall, J. E., 1978. in Membrane Transport in Biology (Giebisch, G., Tosteson, D. C. and Ussing, H. H., eds.) Vol. 1, pp. 475–531, Springer-Verlag, Berlin.
101. Latorre, R., Alvarez, O. and Hall, J. E., 1976. Biophys. J. 16: 80a.
102. Szabo, G., 1974. Nature 252: 47–49.
103. Latorre, R. and Quay, S., 1981. Biophys. J. 33: 64a.
104. McLaughlin, S. and Eisenberg, M., 1975. Ann. Rev. Biophys. Bioengg. 4: 335–366.
105. Mathew, M. K., Nagaraj, R. and Balaram, P., 1982. J. Membr. Biol. 65: 13–17.
106. Nagaraj, R., Mathew, M. K. and Balaram, P., 1980. FEBS Lett. 121: 365–368.
107. Mitchell, P., 1975. FEBS Lett. 59: 137–139.
108. Boyer, P. D., Chance, B., Ernster, L., Mitchell, P., Racker, E. and Slater, E. C., 1977. Ann. Rev. Biochem. 46: 955–1026.
109. Montal, M., Chance, B. and Lee, C.-P., 1970. J. Membr. Biol. 2: 201–234.
110. Green, D. E. and Vande Zande, H., 1981. Biochem. Biophys. Res. Commun. 100: 1017–1024.
111. Takaishi, Y., Terada, H. and Fujita, T., 1980. Experientia 36: 550–552.
112. Mathew, M. K., Nagaraj, R. and Balaram, P., 1981. Biochem. Biophys. Res. Commun. 98: 548–555.
113. Mathew, M. K., Nagaraj, R. and Balaram, P., 1981. Biochim. Biophys. Acta 649: 336–342.
114. Mathew, M. K., Nagaraj, R. and Balaram, P., 1982. J. Biol. Chem., 257: 2170–2177.
115. Nagaraj, R. and Balaram, P., 1979. Biochem. Biophys. Res. Commun. 89: 1041–1049.
116. McMullen, A. I. and Stirrup, J. A., 1971. Biochim. Biophys. Acta 241: 807–814.
117. Corkill, J. M., Goodman, J. F., Robson, P. and Tate, J. R., 1966. Trans. Faraday Soc. 62: 987–993.
118. Tanford, C., 1973. The Hydrophobic Effect: Formation of Micelles and Biological Membranes, Wiley, N.Y.
119. Schindler, H. and Rosenbusch, J. P., 1981. Proc. Natl. Acad. Sci. (USA) 78: 2302–2306.

120. Stankowski, S. and Gruenwald, B., 1980. Biophys. Chem. 12: 167–176.
121. Mukerjee, P., 1962. J. Phys. Chem. 66: 943–945.
122. Birdi, K. S., Dulsager, S. U. and Bäcklund, S., 1980. J. Chem. Soc. Faraday I, 76: 3403–3407.
123. Boheim, G., Hanke, W. and Eibl, H., 1980. Proc. Natl. Acad. Sci. (USA), 77: 3403–3407.
124. Ermishkin, L. N., Kasumov, Kh. M. and Potseluyev, V. M., 1977. Biochim. Biophys. Acta 470: 357–367.
125. Urry, D. W., 1972. Biochim. Biophys. Acta 265: 115–168.
126. Vodyanoy, I., Hall, J. E., Balasubramanian, T. M. and Marshall, G. R., 1982. Biochim. Biophys. Acta 684: 53–58.
127. Latorre, R. and Donovan, J. J., 1980. Acta Physiol. Scand. Suppl. 481: 37–45.
128. Chapman, D., Cherry, R. J., Finer, E. G., Hauser, H., Phillips, M. C., Shipley, G. G. and McMullen, A. I., 1969. Nature 224: 692–694.
129. Gisin, B. F., Kobayashi, S. and Hall, J. E., 1977. Proc. Natl. Acad. Sci. (USA) 74: 115–119.
130. Wada, A., 1976. Adv. Biophys. 9: 1–63.
131. Hol, W. G. J., Halie, L. M. and Sander, C., 1981. Nature 294: 532–536.
132. Hol, W. G. J., van Duijnen, P. Th. and Berendsen, H. J. C., 1978. Nature 273: 443–446.
133. Yantorno, R. E., Takashima, S. and Mueller, P., 1977. Biophys. J. 17: 87a.
134. Urry, D. W., 1975. Int. J. Quantum Chem. Quantum Biol. Symp. 2: 221–235.
135. Schwarz, G., 1978. J. Membr. Biol. 43: 127–148.
136. Fringeli, U. P. and Fringeli, M., 1979. Proc. Natl. Acad. Sci. (USA), 76: 3852–3856.
137. Fringeli, U. P., 1980. J. Membr. Biol. 54: 203–212.
138. Schindler, H., 1979. FEBS Letters 104: 157–160.
139. McIntosh, T. J., Ting-Beall, H. P. and Zampighi, G., 1982. Biochim. Biophys. Acta 685: 51–60.
140. Koeppe, R. E., Berg, J. M., Hodgson, K. O. and Stryer, L., 1979. Nature 279: 723–725.
141. Baumann, G., 1981. Biophys. J. 35: 699–705.
142. Urry, D. W., Prasad, K. U. and Trapane, T. L., 1982. Proc. Natl. Acad. Sci. (USA) 79: 390–394.
143. Frank, H. S. and Evans, M. W., 1945. J. Chem. Phys. 13: 507–532.
144. Edmonds, D. T., 1981. Trends Biochem. Sci. 6: 92–94.
145. Stanfield, P. R., Ashcroft, F. M. and Plant, T. D., 1981. Nature 289: 509–511.
146. Frelin, C., Vigne, P. and Lazdunski, M., 1981. Eur. J. Biochem. 119: 437–442.
147. Eigen, M. and De Maeyer, L., 1958. Proc. Roy. Soc. London, Ser A, 247: 505–533.
148. Williams, R. J. P., 1975. Electron Transfer Chains and Oxidative Phosphorylation (Quagliariello, E., Papa, S., Palmieri, F., Slater, E. C. and Siliprandi, N., eds.) pp. 417–422, North-Holland Publishing Co., Amsterdam.
149. Nichols, J. W. and Deamer, D. W., 1980. Proc. Natl. Acad. Sci. (USA) 77: 2038–2042.
150. Biegel, C. M. and Gould, J. M., 1981. Biochemistry 20: 3474–3479.
151. Karle, I. L., 1977. J. Am. Chem. Soc. 99: 5152–5157.
152. Rao, Ch. P., Shamala, N., Nagaraj, R., Rao, C. N. R. and Balaram, P., 1981. Biochem. Biophys. Res. Commun. 103: 898–904.
153. Engelman, D. M. and Steitz, T. A., 1981. Cell 23: 411–422.
154. Unwin, P. N. T. and Henderson, R., 1975. J. Mol. Biol. 94: 425–440.
155. Bruckner, H., Jung, G., Hanke, W. and Boheim, G., 1979. Abstracts of the Annual Meeting of the Deutsche Gesellschaft fur Biophysik, Konstanz, Abstract B33, p. 55.
156. Donovan, J. J., Simon, M. I., Draper, R. K. and Montal, M., 1981. Proc. Natl. Acad. Sci. (USA) 78: 172–176.
157. Kagan, B. L., Finkelstein, A. and Columbini, M., 1981. Proc. Natl. Acad. Sci. (USA) 78: 4950–4954.
158. Benz, R., Janko, K. and Lauger, P., 1980. Ann. N.Y. Acad. Sci. 358: 13–24.
159. Hille, B., 1971. J. Gen Physiol. 58: 599–619.
160. Hille, B., 1973. J. Gen. Physiol. 61: 669–686.
161. Schwarzmann, G., Wiegandt, H., Rose, B., Zimmerman, A., Ben-Haim, D. and Loewenstein, W. R., 1981. Science 213: 551–553.
162. Benz, R. and Hancock, R. E. W., 1981. Biochim. Biophys. Acta 646: 298–308.
163. Boehler-Kohler, B. A., Boos, W., Dieterle, R. and Benz, R., 1979. J. Bacteriol. 138: 33–39.
164. Benz, R., Ishii, J. and Nakae, T., 1980. J. Membr. Biol. 56: 19–29.

Received 25 May 1982.